

X-52198
(NASA-TM-~~76923~~) STORABLE PROPELLANT
COMBUSTION INSTABILITY PROGRAM AT LEWIS
RESEARCH CENTER (NASA) 31 P LIMIT
GOVT. + CONTR.

X77-79024

00/28 Unclas
33415

STORABLE PROPELLANT COMBUSTION INSTABILITY
PROGRAM AT LEWIS RESEARCH CENTER

by William K. Tabata, Robert J. Antl,

and David W. Vincent

Lewis Research Center
Cleveland, Ohio

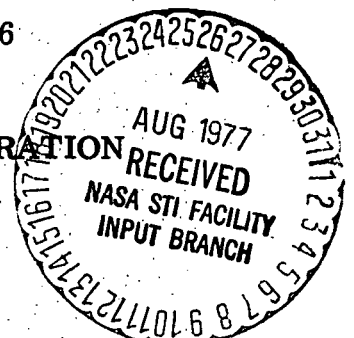
Available to NASA Offices and
Research Centers Only.

| | | |
|-------------------|-------------------------------|------------|
| FACILITY FORM 802 | X66-36923 | |
| | (ACCESSION NUMBER) | |
| | 31 | (THRU) |
| | (PAGES) | 2A |
| | TMX-52198 | (CODE) |
| | (NASA CR OR TMX OR AD NUMBER) | 28 |
| | | (CATEGORY) |

TECHNICAL PAPER proposed for presentation at

Second Propulsion Joint Specialist Conference
sponsored by the American Institute of Aeronautics and Astronautics
Colorado Springs, Colorado, June 13-17, 1966

NATIONAL AERONAUTICS AND SPACE ADMINISTRATION



STORABLE PROPELLANT COMBUSTION INSTABILITY

PROGRAM AT LEWIS RESEARCH CENTER

by William K. Tabata, Robert J. Antl,

and David W. Vincent

Lewis Research Center
National Aeronautics and Space Administration
Cleveland, Ohio

ABSTRACT

An experimental program at Lewis Research Center investigates acoustical-mode combustion instability in liquid propellant rockets. One phase of this program is concerned with nitrogen tetroxide and a 50-50 fuel blend of hydrazine-UDMH. Effects on combustor stability and performance by variations in injection velocities, impingement angle and distance, and thrust per element of triplet injectors were studied in a 10.77-inch-diameter cylindrical combustor at chamber pressures of 100 and 300 psia. Nominal thrust levels were 6700 and 20 000 pounds. Stability rating was accomplished by the use of various size RDX explosive charges to generate tangential pressure disturbances. The injection velocity effect correlated by using a ratio V_o/V_f . Stability correlation with V_o/V_f resulted in a sharply humped curve with maximum stability at a ratio of 1.2. Performance decreased with increase in V_o/V_f after a maximum at 0.7, which agreed fairly well with the "uniform mixture ratio distribution" criteria of the Jet Propulsion Laboratory. Variation of impingement angle from 38° to 120° indicated that performance correlated with the absolute velocity ratio V_o/V_f , but stability correlation appeared to be best with a velocity ratio using the radial component of the fuel injection velocity V_o/V_{fr} . Impingement distances from 0.5 to 1.0 inch appeared to have only slight effect on stability and performance. Investigation of injector thrust per element for V_o/V_{fr} ranging from 0.8 to 2.8 yielded convex maxima curves. Acoustic liners were also tested to improve a liner design computer program, to obtain design criteria, and to develop flight-type liners. A marginally

X-52198

Available to NASA Offices and
Research Centers Only.

E-3445.

stable and a spontaneously unstable combustor were used to evaluate liner configurations. All liners were effective in the marginally stable configuration, and only liners with large theoretical absorptivity were successful in the spontaneously unstable combustor.

INTRODUCTION

An experimental study of storable-propellant acoustical-mode combustion instability was conducted in the Propulsion Sciences Laboratory as part of an extensive program at Lewis Research Center investigating systematically the effects of injection variables on combustion instability in liquid propellant rockets. A propellant combination of nitrogen tetroxide and 50-50 fuel blend of hydrazine-UDMH was used in this phase of the program. The type of injector element tested was the coplanar-unlike-triplet, which has demonstrated high performance capabilities with this propellant combination.¹

Effects of the injection variables, which are injection velocities, impingement angle, impingement distance, and thrust per element, on rocket motor stability and performance were studied in a 10.77-inch-diameter cylindrical combustor at chamber pressures of 100 and 300 psia over a mixture ratio range of 1.4 to 2.2. The nominal thrust levels corresponding to the two chamber pressures were 6700 and 20 000 pounds. The range of variables investigated are presented in Table I.

As a means of remedying combustion instability, several heat-sink acoustic liner configurations were also tested in the program at a chamber pressure of 100 psia and mixture ratios of 2.0 and 1.6. The acoustic liners were tested with a spontaneously unstable and a marginally stable combustor to prove the relative effectiveness of the designs in improving an acoustic liner design computer program, obtaining design criteria, and developing flight-type liners.

Stability rating the various injector and liner configurations was accomplished by subjecting the combustor to tangential pressure pulses generated by various size RDX explosive charges. The RDX charges, or bombs, were detonated in tangential ports in the heat-sink combustion chamber wall during the steady-state portion of the test firings. Reproducibility of the RDX bomb pressure disturbance was good and the RDX bombs proved to be satisfactory as a stability rating technique.

APPARATUS

Combustor

The heat-sink rocket combustor (Fig. 1) used in the injection variables studies was comprised of an injector, a bomb ring, a cylindrical spool piece, and a convergent-divergent exhaust nozzle with a contraction ratio of 1.89 and a nominal throat area of 48 square inches. The chamber had an inside diameter of 10.77 inches, and the distance from the injector to nozzle throat was kept constant at 23.5 inches, which resulted in a constant characteristic length L^* of 42 inches. The inside surfaces of the mild steel chamber and exhaust nozzle were coated with 0.012 inch of nichrome and then with 0.018 inch of flame-sprayed zirconium oxide, which permitted firings of 3.8 seconds duration at chamber pressures of 100 and 300 psia without excessive erosion.

All liners were tested with two combustor configurations utilizing the same injector, which had 487 triplet elements. The configurations were (a) the 487 element triplet with an L^* of 42-inch chamber, which was stable but could be driven unstable by a RDX bomb, and (b) the same injector with an L^* of 56-inch chamber, which was spontaneously unstable from ignition.

The exhaust nozzle had an expansion ratio of 1.3 since test objectives did not require a large area ratio, and the nozzle losses were more accurately predicatable for performance calculations.¹

Injector

All injectors were tested as fuel-oxidant-fuel triplets at a chamber

pressure of 300 psia and also 100 psia, if the injection differential pressures were sufficiently large to ensure no "chugging-type" instability. Several of the configurations were also tested as oxidant-fuel-oxidant triplets. Injectors were flat-faced and the orifice length-to-diameter ratios varied from a maximum of 12.5 to a minimum of 6.0.

In addition to the injection variables listed in Table I, two types of injection patterns (Fig. 2) were tested to determine the effect of pattern layout. In one case, the triplet elements were arranged in concentric rings (Figs. 2(a) and (b)), and the resultant impingement fans were all parallel to the chamber wall, whereas the second pattern was an alternating-grid (Fig. 2 (c)) that had adjacent impingement fans normal to each other.

Acoustic Liners

The heat-sink, perforated acoustic liners tested (Fig. 3) were 0.1875 inch thick, made of mild steel, and flame-sprayed with zirconium oxide. Aperture diameters were either 0.125 or 0.25 inch, and the open area ranged from 2.5 to 20.0 percent. Open area was calculated by summing the area of the apertures in 1 square inch of the liner surface area. The resonator cavity behind the liners was 0.97 inch deep, and the axial length varied from 10.0 to 2.5 inches. Two slotted liners and one cross liner 0.1875 inch thick were also tested to study the effect of the aperture shape (Fig. 4). The slots were either 0.0625 or 0.125 inch wide and ran the length of the 10.0-inch liner resulting in open areas of 5 and 10 percent. The cross liner had arms 0.125 inch wide and a 10-percent open area. All liners had three circumferential partitions similar to those shown in Figs. 3 and 4, which separated the resonator cavity into four compartments.

RDX Explosive Bombs

The heat-sink bomb ring shown in Fig. 1 constituted a segment of the chamber and permitted detonating RDX explosive (MIL-R-398) bombs, which ranged in size from 1.6 to 45.2 grains, in the four tangential ports during the

steady-state portion of a test firing. In order to eliminate the variables of bomb location and direction, the bomb ring was adjacent to the injector for all injection variables tests, and the direction of the bomb ports was always counterclockwise as viewed upstream. The centerline of the ports was tangent to a circle 2 inches less in diameter than the combustion chamber inside diameter.

The RDX bomb (Fig. 5) had an initiator consisting of an exploding bridge-wire (EBW) and 1.6 grains of PETN (pentaerythrite tetranitrate, MIL-P-387A) explosive to which were added various amounts of RDX explosive. A voltage greater than 2000 volts was required to initiate the bombs; therefore, stray RF signals or static electric charges could not accidentally cause a detonation. PETN has brisance characteristic very similar to RDX, but it is easier to detonate electrically and, for this reason, was employed in the initiator. The RDX was 98-percent RDX and 2-percent steric acid, molded in tablets 0.10 inch thick, 0.368 inch in diameter, and containing 4.4 grains. Bomb size could be changed simply by varying the number of RDX tablets assembled with the initiator. The bomb was insulated from the hot combustion gases by a plastic cap, and the assembly was placed 1.0 inch from the chamber inside surface in one of the bomb ports. Reliability of these bombs was good, although a small percentage of the bombs did not detonate as programmed because of low voltage.

Test Facility

Test objectives did not require an altitude capability, but a Lewis altitude facility was used in order to handle the toxic exhaust gases and any propellant spills that might occur. The propellant temperature was 65±11 °F throughout the test program. No attempt was made to reduce further this temperature variation.

Instrumentation

The combustor and the facility were instrumented to record and monitor the normal operating parameters. Included were propellant tank pressures and

temperatures, propellant flow rates, injection pressures and temperatures, combustion chamber pressure, combustor thrust, and ambient conditions. Pressure measurements were obtained by strain-gage-type transducers, and temperatures were measured by iron-constantan thermocouples. Flow rates were indicated by turbine flowmeters.

High-frequency piezoelectric pressure transducers in water-cooled jackets, having a response flat to 6000 cps as installed, were mounted flush to the combustion chamber wall as shown in Fig. 1. The three locations on the combustion chamber provided a means to determine the frequency and phase relation of pressure oscillations that facilitated identification of the modes of instability.

Combustor and facility operating parameters were recorded on an oscillograph located in the facility control room and on a digital data recorder for computer processing. The data from the high-frequency pressure transducers and a signal to indicate the initiation of the RDX bombs were recorded on magnetic tape.

PROCEDURE

Each injector or liner configuration was mounted in the test stand and four RDX bombs of increasing grain size were placed in the four tangential bomb ports. Program timers were used to sequence operation of the fuel and oxidizer control valves for a 2.8- to 3.8-second firing and to sequence the firing of the four RDX bombs in a given order during the steady-state portion of the test at intervals of 100 milliseconds. An electronic controller regulated fuel and oxidizer mass flow rates, and in this manner the chamber pressure and the mixture ratio were maintained constant throughout the firing.

Analysis of the data from the high-frequency pressure transducers, transferred from the magnetic tape onto an oscillograph at a slower tape speed, determined which RDX bombs detonated and were damped, which RDX bomb drove the combustor into a sustained instability, and a first estimate of the modes and amplitudes of the resulting instability. These data were later processed on a spectrum analyzer to obtain more exact frequency and amplitude analysis.

RESULTS AND DISCUSSION

The results of the various phases of this investigation are presented in forms of cross-plots in Figs. 8 to 11; that is, stability and performance data for each configuration tested were first plotted as a function of mixture ratio, and then values at nominal mixture ratios of 1.6 and 2.0 and chamber pressures of 100 and 300 psia were plotted as a function of the variables under investigation.

A brief description of the stability rating technique utilizing the RDX explosive bombs is presented herein followed by the discussion of the injection velocity, impingement angle and distance, and thrust per element effects on combustor stability and performance. This section is concluded with an explanation of the attempts to obtain an empirical relation between the injection variables and stability and finally a discussion of the acoustic liner test results.

Stability Rating Technique

As discussed earlier, the method employed to initiate high-frequency combustion instability was the detonation of various size RDX explosive bombs in tangential ports in the combustion chamber wall. Attempts to use the initial or maximum pressure spikes (which were usually not one and the same) produced by the bombs proved to be an unsatisfactory stability rating scale. A chemical augmentation by the combustion process, similar to the augmentation of pressure waves discussed in Ref. 2, masked the actual pressure disturbances created by the bombs resulting in large data scatter. This effect is illustrated graphically by comparing the hot firing and cold (helium-pressurized chamber) maximum pressure spikes as a function of bomb size presented in Fig. 6. The cold bomb data for chamber pressures of 100 and 300 psia resulted in two 5- to 15-psi-wide bands, which ranged from a mean value of 10 to 80 psi as grain size varied from 1.6 to 41.0 grains. The hot-firing bomb data plotted for several runs yielded one band of 50 to 75 psi for both chamber pressures with mean values of 58 psi for 1.6 grains and 190 psi for 32.2 grains. Chemical augmentation

was probably the first cycle of an instability that either damped or became cyclic.

The size of the explosive bomb was used, therefore, as a stability rating scale. It was noted that, for a given injector configuration, chamber pressure, and mixture ratio, instability was repeatedly initiated by a particular bomb size. Relative stability will be described in terms of the minimum bomb size (in grains) required to induce a sustained high-frequency combustion instability in the combustor.

Injection Velocity Effects

Results of the liquid oxygen - hydrogen portion of the acoustical-mode combustion instability program at Lewis and tests by others³ have indicated that injection velocity ratio has a strong influence on combustion instability. For the storable propellant study, therefore, wide ranges of injection velocities and velocity ratios were investigated at chamber pressures of 100 and 300 psia and mixture ratios of 1.4 to 2.2 (Fig. 7 and Table I). The range of injection velocity ratios, which was limited by the facility propellant systems, was approximately 0.5 to 2.5. It should be noted that the ratio of oxidizer velocity to fuel velocity V_O/V_F , which is the inverse of the ratio used in the liquid oxygen - hydrogen studies, was employed in this investigation, since the fuel was considered to be the controlling propellant. Calculations based on Ref. 4 indicated the fuel to be the slower to vaporize.

The characteristic exhaust velocity efficiency η_C^* for stable operation and the minimum bomb size required to initiate instability for the injector configurations tested are presented in Fig. 8 as a function of injection velocity ratio. Shown in the figure are cross-plotted data for chamber pressures of 100 and 300 psia at propellant mixture ratios of 1.6 and 2.0. Combustor performance values η_C^* were based on vacuum specific impulse efficiency, as was done in Ref. 1, since this method resulted in better accuracy than the use of measured chamber pressure.

Stability, as shown in Fig. 8, was found to be a function of chamber pressure and injection velocity ratio. Correlations using absolute or differential injection velocities were attempted, but the best correlation appeared to be with a velocity ratio. At a chamber pressure of 100 psia and velocity ratios less than 1.3, the combustor was marginally stable since only the bomb initiator (1.6 grains) was required to promote instability when it was not already spontaneously unstable from ignition. The trend of the data at a larger velocity ratio was toward increased stability. A charge of 6.0 grains was required to induce instability at a velocity ratio of 1.7.

At a chamber pressure of 300 psia, the effect of injection velocity ratio on stability was more pronounced. A narrow band of maximum stability was found between velocity ratios of 1.0 and 1.4 within which bombs as large as 23.4 to 32.2 grains were required to drive the combustor unstable. Bombs of 6.0 to 10.4 grains were sufficient for ratios less than 1.0 or greater than 1.4. An interesting observation was that peak stability occurred at slightly higher velocity ratio than that for peak performance, and the combustors were less stable at maximum and lower levels of performance.

As was the case with stability, performance was a function of chamber pressure and velocity ratio. At a chamber pressure of 100 psia, the performance optimized at approximately 93.5 percent, whereas the peak performance value for a chamber pressure of 300 psia was about 95.6 percent. Optimum performance was obtained for both chamber pressures at an injection velocity ratio of approximately 0.7, which was slightly less than the ratio predicted by the Jet Propulsion Laboratory's "uniform mixture ratio distribution" criteria.⁵ The optimum velocity ratio for the configurations tested, based on the aforementioned criteria, was approximately 0.95. The discrepancy between the predicted and experimental values was possibly due to the "blow-apart" phenomenon postulated for liquid-phase reacting propellants.⁶

The velocity ratio study injectors were primarily tested as fuel-oxidant-fuel triplets. Some of the injectors were also tested as oxidant-fuel-oxidant,

and for identical injection velocity ratios all were found to be less stable and higher performing. Testing of the oxidant-fuel-oxidant triplets ceased early in the test program because they proved to be very erosive to bomb rings, chambers, and nozzles.

Impingement Angle and Distance

The effects of impingement angle and distance were investigated by varying the included impingement angle from the 60° used in the velocity ratio study to 38° and 120° as the impingement distance of 0.5 inch and the injection pattern were kept constant. Then with the 30° and 60° included impingement angles, holding injection pattern and velocity ratio constant, the impingement distance was extended from 0.5 to 1.0 inch from the injector face. The chamber pressure and mixture ratio ranges were again 100 and 300 psia and 1.4 to 2.2.

Effect of impingement angle variation with the 0.5-inch impingement distance is shown in Fig. 9 as a function of V_o/V_f for cross-plotted data at a chamber pressure of 300 psia and mixture ratio of 2.0. Performance continues to indicate a good correlation with absolute injection velocity ratio. The data for the two other angles lie very close to the curve for 60° . Stability data did not corroborate the trend found for 60° , therefore, in order to obtain a stability correlation, the axial and radial components of the fuel injection velocity V_{fa} and V_{fr} were used in the velocity ratio. These data are presented in Fig. 10 with the data from Fig. 8 at a mixture ratio of 2.0. The better correlation appears to be with the radial component of the fuel velocity V_o/V_{fr} , but neither correlation is strong since no configurations employing the 38° and 120° impingement angle were tested with velocity ratios in the band of maximum stability.

Shown also in Fig. 10 is the effect of varying the impingement distance as the impingement angle was kept constant at 30° and 60° . There appears to be only a minor effect for the configurations tested. Performance, which is not presented in the figure, also indicated only a minor effect of impingement distance.

Thrust Per Element

The thrust, or fuel mass flow, per element investigation utilized the 60° impingement angle and nominal 0.5-inch impingement distance. Injectors with 50, 101, 201, and 401 elements arranged in a circular pattern and injectors with 52, 104, and 208 elements arranged in an alternating-grid pattern were tested at chamber pressures of 100 and 300 psia and various injection velocity ratios (Table I and Fig. 2). Cross-plotted data at a mixture ratio of 2.0 are presented in Figs. 11(a) and (b) for chamber pressures of 100 and 300 psia.

For circular patterns, at a nominal velocity ratio of 1.8, and chamber pressures of 100 and 300 psia, the data resulted in convex maxima curves; that is, stability and performance increased to a maximum and then decreased as fuel mass flow per element increased. Performance trends were similar at a velocity ratio of 2.8 and chamber pressure of 300 psia, but stability was different. Stability continued to increase with increase in W_f/E with a possible maximum at a larger value of W_f/E than tested. An interrelation between V_o/V_{fr} and W_f/E is apparent and in order to obtain maximum stability and performance, it may be necessary to select proper combinations of V_o/V_{fr} and W_f/E .

The alternating-grid injection pattern resulted in a decrease in maximum stability and a 1 to 2 percent increase in performance compared with that of the circular pattern, as seen in Fig. 11. It is believed that the "blow-apart" phenomenon and the alternating fans that would produce a second mixing zone are the reasons for the improved performance and subsequent reduced stability.

Attention should be brought to the fact that maximum stability for the thrust per element study was not as great as that encountered in the velocity ratio investigation. There are two possible explanations for this anomaly, namely (a) that the thrust per element configurations were not tested in the maximum stability band since the interrelation between V_o/V_{fr} and W_f/E was unknown and (b) that the difference in circular injection patterns used in the two investigations had an effect. Comparison of the two patterns is shown in Fig. 2. The 90-element circular pattern (Fig. 2(a)) used in the V_o/V_{fr} study

had elements in a slightly nonuniform area distribution so that the angle and distance variations could be made without altering the location of the center orifice of the triplet element (normally oxidizer orifice). The injection patterns for the thrust per element investigation (two of which are shown in Figs. 2(b) and (c)) were distributed uniformly over the injector face area. The distribution variations are not as drastic as those reported in Refs. 7 and 8, but the differences could still have accounted for the change in stability characteristics.

Stability Correlation

An analytical explanation of why stability should correlate with V_o/V_{fr} or W_f/E will not be attempted herein, but it should be noted that the parameters could be modified to suggest physical processes such as liquid jet rigidity, vaporization, and so forth.

Attempts, as yet incomplete, are being made to correlate the injection velocity ratio and the thrust per element data and to determine the chamber pressure effect with the aid of several combustion instability theories.^{9,10} It was noted in these investigations that the mode of the generated instability shifted from the first radial or second tangential to the first tangential as velocity ratio and fuel mass flow per element were increased. It appears that a correlation of V_o/V_{fr} , W_f/E , and chamber pressure effects with Crocco's sensitive time lag or Priem's burning rate parameter may be possible.

Acoustic Liners

A Pratt & Whitney computer program based on Helmholtz resonator theory was used to design several acoustic liners that showed promise of damping the acoustical-mode instability encountered with the two particular combustor configurations tested in this phase of the program. Spectrum analysis indicated the modes of instability exhibited by both configurations to be primarily the first radial (4950 cps) with lower amplitude first and second tangential (2400 and 3950 cps) and discrete high-order longitudinal modes. Combustor operating conditions were a chamber pressure of 100 psia and mixture ratios of 2.0 and 1.6.

All perforated liner configurations tested (Table II) in the marginally stable combustor ($L^* = 42$ in.) were successful in damping the largest RDX bombs possible to test (45.2 grains), which produced pressure disturbances as large as 100 to 180 psi (peak-to-peak). Without a liner, 10.4 grains or pressure disturbances of 35 to 65 psi (peak-to-peak) would drive the combustor unstable. For the spontaneously unstable combustor that utilized the same injector with a chamber having an L^* of 56 inches, only four liner configurations were successful. To ensure that the larger L^* of the spontaneously unstable combustor (smaller ratio of liner surface area to total chamber surface area for constant length liners) was not the reason why half of the liner configurations did not damp the instability, several unsuccessful liners were tested with spontaneously unstable injector/chamber configurations from the injection variables investigation. These configurations all had an L^* of 42 inches, similar to the marginally stable combustor for the liner study. Test results were identical to that of the L^* configuration of 56 inches; that is, instability was not completely suppressed.

An input to the computer program for liner design is the backing temperature, or the temperature of the gases behind the liner. For a given combustor, this temperature varied with the size of the liner holes and the percent open area. By using the measured temperatures, the operating band on the theoretical absorption curves for the liners tested could be determined as shown in Fig. 12.

The theoretical absorptivity (calculated for the first radial mode) of the liners tested varied from 0.05 to 0.70. All liners damped the marginally stable combustor. With the spontaneously unstable combustor, only liner configurations with a theoretical absorptivity of 0.30 or greater were successful. It can be concluded that, for a marginally stable combustor, practically any liner design will damp the instability, but with a spontaneously unstable combustor, only liners with large values of theoretical absorptivity will be successful.

Liner position and length were found to be important factors. For the tangential modes, the liner should be placed adjacent to the injector. Minimum

liner length was also indicated, but data gathered do not define exactly the minimum effective length and what function it is of injection variables or instability modes.

The slotted and cross liners tested to determine the effect of hole shape on absorption characteristics demonstrated results similar to the round-hole, perforated liners. It appears initially that hole shape does not have a first-order effect on liner effectiveness.

Several flight-type liners for use with engines employing ablative cooling are being designed from the heat-sink liner test results for experimental evaluation. They include a ceramic liner made of zirconium oxide, a refractory metal liner, and an ablative liner. In addition, a regeneratively cooled liner is in the design stage.

SUMMARY

Combustors, injectors, and liners were tested at chamber pressures of 100 and 300 psia, at mixture ratios of 1.4 to 2.2, and in a 10.77-inch-diameter cylindrical combustor with a contraction ratio of 1.89. The following results were obtained:

1. Performance was found to be a function of injection velocity ratio V_o/V_f and maximized at a ratio slightly less than that predicted by the Jet Propulsion Laboratory's "uniform mixture ratio distribution" criteria.
2. Acoustical-mode combustion instability was affected by injection velocity ratio and appeared to correlate with a ratio employing the radial component of the fuel injection velocity V_o/V_{fr} with a narrow band of maximum stability that occurs near maximum performance.
3. Impingement distance appeared to have only a slight effect on stability and performance for the few configurations tested.
4. Thrust, or fuel mass flow, per element variation at various velocity ratios indicated an interrelation between W_f/E and V_o/V_{fr} and, in order to obtain maximum stability and performance, a proper selection of both is necessary.
5. A fuel-oxidant-fuel coplanar triplet was more stable but less efficient

than the oxidant-fuel-oxidant triplet.

6. An alternating-grid injection pattern was more efficient but less stable than a circular injection pattern.

7. Acoustic liners tested were very effective for damping acoustical-mode combustion instability in that practically any liner design stabilized a marginally stable combustor and a good liner design (theoretical absorptivity greater than 0.30) stabilized a spontaneously unstable combustor.

REFERENCES

1. Aukerman, Carl A. and Trout, Arthur M.: Experimental Rocket Performance of the Apollo Storable Propellants in Engines with Large Area Ratio Nozzles. Proposed NASA TN.
2. Nicholls, J.A., Dabora, E.K., and Ragland, K.W., "A Study of Two Phase Detonation as It Relates to Rocket Motor Combustion Instability," NASA CR-272 (August 1965).
3. Wanhainen, John P., Parish, Harold C., and Conrad, E. William: Effects of Injection Velocities on Screech in 20 000-Pound Hydrogen-Oxygen Rocket. Proposed NASA TN.
4. Priem, R.J. and Heidmann, M.F., "Propellant Vaporization as a Design Criterion for Rocket-Engine Combustion Chambers," NASA TR R-67 (1960).
5. Elverum, G.W. Jr., and Morey, T.F., "Criteria for Optimum Mixture-Ratio Distribution Using Several Types of Impinging-Stream Injector Elements," N-73207X Calif. Inst. Tech., Jet Prop. Lab., Memo. 30-5 (February 1959).
6. Rupe, J.H. and Evans, D.D., "Designing for Compatability in High-Performance LP Engines," *Astronautics and Aeronautics* 3, 68-74 (June 1965).
7. Osborn, J.R. and Davis, L.R., "Effects of Injection Location in Combustion Instability in Premixed Gaseous Bipropellant Rocket Motors," N-94833 Purdue University, Report No. I-61-1 (January 1961).

8. Reardon, F.H., McBride, J.M., and Smith, A.J., Jr., "Effect of Injection Distribution on Combustion Stability," AIAA J. 4, 506-512 (1966).
9. Crocco, L. and Cheng, S.I., Theory of Combustion Instability in Liquid Propellant Rocket Motors, AGARDograph No. 8 (Butterworth Scientific Publications, Ltd., London, 1956).
10. Priem, R.J., "Combustion Process Influence on Stability," presented at the 55th National Meeting, A.I.Ch.E., San Francisco, May 16-19, 1965.

TABLE I. - EXPERIMENTAL INJECTOR DESIGN POINTS

[Mixture ratio, 2.0; C* efficiency, 95 percent; fuel density, 56.4 lb/ft³; oxidizer density, 90.2 lb/ft³]

| Investigation | Impingement | | Injection velocity | | Chamber pressure, P _c , psia | Velocity ratio, V _o /V _f | Thrust-element ratio, T/E, lb/E | Fuel-element ratio, W _f /E, lb/secE | Pattern | Number of elements |
|--------------------|-------------|---------------|-------------------------|-------------------------|---|--|---------------------------------|--|----------|--------------------|
| | Angle, deg | Distance, in. | V _o , ft/sec | V _f , ft/sec | | | | | | |
| Injection velocity | 60 | 0.5 | 108 | 65 | 100 | 1.66 | 74 | 0.108 | Circular | 90 |
| | | | 82 | 65 | | 1.26 | | | | |
| | | | 59 | 65 | | .91 | | | | |
| | | | 40 | 65 | | .62 | | | | |
| | | | 40 | 45 | | .89 | | | | |
| | | | 243 | 192 | 300 | 1.27 | 222 | .319 | | |
| | | | 175 | 192 | | .91 | | | | |
| | | | 120 | 192 | | .63 | | | | |
| | | | 120 | 133 | | .90 | | | | |
| | | | 120 | 97 | | 1.24 | | | | |
| | | | 120 | 70 | | 1.72 | | | | |
| | | | 243 | 133 | | 1.83 | | | | |
| | | | 243 | 97 | | 2.51 | | | | |
| | | | 175 | 97 | | 1.81 | | | | |
| 96 | 97 | | .99 | | | | | | | |
| Impingement angle | 120 | 0.5 | 108 | 65 | 100 | 1.66 | 74 | 0.108 | Circular | 90 |
| | | | 82 | 65 | 100 | 1.26 | 74 | .108 | | |
| | | | 59 | 65 | 100 | .91 | 74 | .108 | | |
| | | | 82 | 45 | 100 | 1.82 | 74 | .108 | | |
| | | | 243 | 133 | 300 | 1.83 | 222 | .319 | | |
| | | | 243 | 97 | | 2.51 | | | | |
| | | | 96 | 97 | | .99 | | | | |
| | | | 96 | 65 | | 1.48 | | | | |
| | | | 96 | 70 | | 1.37 | | | | |
| | | | 82 | 65 | 100 | 1.26 | 74 | .108 | | |
| | | | 59 | 65 | 100 | .91 | 74 | .108 | | |
| | | | 108 | 45 | 100 | 2.40 | 74 | .108 | | |
| | | | 243 | 192 | 300 | 1.27 | 222 | .319 | | |
| | | | 175 | 192 | | .91 | | | | |
| 243 | 97 | | 2.51 | | | | | | | |
| 175 | 97 | | 1.81 | | | | | | | |
| 96 | 97 | | .99 | | | | | | | |
| 96 | 192 | | .50 | | | | | | | |
| 96 | 70 | | 1.37 | | | | | | | |

| | | | | | | | | | | |
|--------------------------------|----|-----|-----|-----|-----|------|-----|-------|----------|-----|
| Impingement distance | 60 | 1.0 | 59 | 65 | 100 | 0.91 | 74 | 0.108 | Circular | 90 |
| | 60 | 1.5 | 59 | 65 | 100 | .91 | 74 | .108 | | |
| | 30 | 1.0 | 59 | 65 | 100 | .91 | 74 | .108 | | |
| | 30 | 1.5 | 59 | 65 | 100 | .91 | 74 | .108 | | |
| | 60 | 1.0 | 96 | 97 | 300 | .99 | 222 | .319 | | |
| | 60 | 1.5 | 96 | 97 | 300 | .99 | 222 | .319 | | |
| | 30 | 1.0 | 96 | 97 | 300 | .99 | 222 | .319 | | |
| | 30 | 1.5 | 96 | 97 | 300 | .99 | 222 | .319 | | |
| Pattern and thrust per element | 60 | 0.5 | 47 | 53 | 100 | 0.89 | 133 | 0.194 | Circular | 50 |
| | | | 47 | 53 | 100 | .89 | 66 | .096 | | 101 |
| | | | 47 | 53 | 100 | .89 | 33 | .048 | | 201 |
| | | | 47 | 53 | 100 | .89 | 17 | .024 | | 401 |
| | | | 138 | 158 | 300 | .87 | 400 | .574 | | 50 |
| | | | 138 | 97 | | 1.42 | 400 | .574 | | |
| | | | 90 | 97 | | .93 | 400 | .574 | | |
| | | | 68 | 97 | | .70 | 400 | .574 | | |
| | | | 138 | 158 | | .87 | 198 | .284 | | 101 |
| | | | 138 | 102 | | 1.35 | 198 | .284 | | |
| | | | 86 | 102 | | .84 | 198 | .284 | | |
| | | | 70 | 102 | | .69 | 198 | .284 | | |
| | | | 138 | 158 | | .87 | 100 | .143 | | 201 |
| | | | 138 | 106 | | 1.30 | 100 | .143 | | |
| | | | 86 | 106 | | .81 | 100 | .143 | | |
| | | | 67 | 106 | | .63 | 100 | .143 | | |
| | | | 138 | 158 | | .87 | 50 | .072 | | 401 |
| | | | 138 | 106 | | 1.30 | 50 | .072 | | |
| | | | 96 | 106 | | .91 | 50 | .072 | | |
| | | | 72 | 106 | | .68 | 50 | .072 | | |
| | | | 82 | 67 | 100 | 1.22 | 128 | .187 | Grid | 52 |
| | | | 56 | 67 | | .84 | 128 | .187 | | 52 |
| | | | 41 | 67 | | .61 | 128 | .187 | | 52 |
| | | | 84 | 69 | | 1.22 | 64 | .093 | | 104 |
| | | | 56 | 69 | | .81 | 64 | .093 | | 104 |
| | | | 41 | 69 | | 0.59 | 64 | .093 | | 104 |
| | | | 86 | 62 | | 1.39 | 32 | .047 | | 208 |
| | | | 54 | 62 | | .87 | 32 | .047 | | 208 |
| | | | 42 | 62 | | .68 | 32 | .047 | | 208 |
| | | | 166 | 200 | 300 | .83 | 385 | .552 | | 52 |
| | | | 121 | 200 | | .60 | 385 | .552 | | 52 |
| | | | 86 | 200 | | .43 | 385 | .552 | | 52 |
| | | | 167 | 204 | | .82 | 192 | .276 | | 104 |
| | | | 121 | 204 | | .59 | 192 | .276 | | 104 |
| | | | 83 | 204 | | .41 | 192 | .276 | | 104 |
| | | | 159 | 183 | | .87 | 96 | .138 | | 208 |
| | | | 124 | 183 | | .68 | 96 | .138 | | 208 |
| | | | 85 | 183 | | .46 | 96 | .138 | | 208 |

TABLE II. - ACOUSTIC LINER RESULTS

[Heat sink, 0.1875 in. thick; nominal operating conditions: P_c , 100 psia; O/F, 2.0 and 1.6]

| | | Combusitor | | |
|----------------|--------------------|-------------|---|--|
| Hole size, in. | Open area, percent | Length, in. | Marginally stable* | Spontaneously unstable** |
| 0.125 | 10 | 10 | Damped 45.2 grains RDX with pressure spikes of 100 to 180 psi peak-to-peak ↓ | Damped transverse modes |
| | 10 | 5 | | Transverse or longitudinal modes not damped |
| | 10 | 2.5 | | Transverse or longitudinal modes not damped |
| | 5 | 10 | | Transverse or longitudinal modes not damped |
| 0.25 | 20 | 10 | Damped 45.2 grains RDX with pressure spikes of 100 to 180 psi peak-to-peak | Damped transverse modes |
| | 10 | 10 | Damped 45.2 grains RDX with pressure spikes of 100 to 180 psi peak-to-peak | Damped transverse modes at O/F of 2.0 but not at 1.6 |
| | 10 | 5 | Damped 45.2 grains RDX with pressure spikes of 100 to 180 psi peak-to-peak | Damped transverse modes at O/F of 2.0 but not at 1.6 |
| | 5 | 10 | Damped 45.2 grains RDX with pressure spikes of 100 to 200 psi peak-to-peak at O/F of 2.0, but 45.2 grains RDX drove into first tangential at O/F of 1.6 | Did not damp transverse or longitudinal modes. |

Characteristic length L^ , 42 in.

**Characteristic length L^* , 56 in.

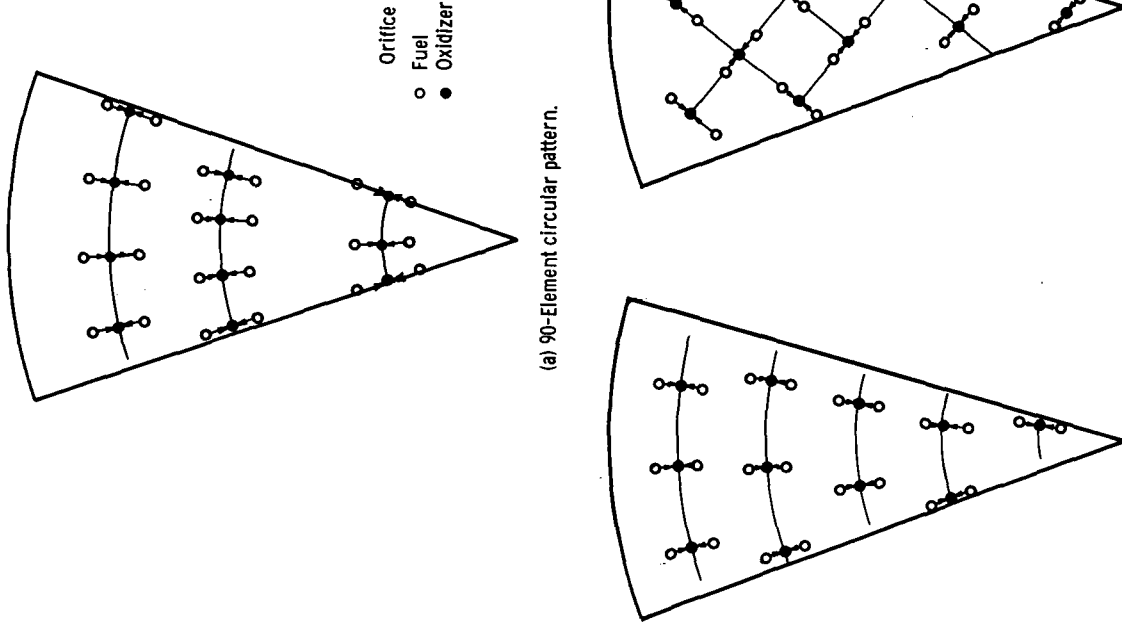


Figure 2. - Section of injector face of patterns.

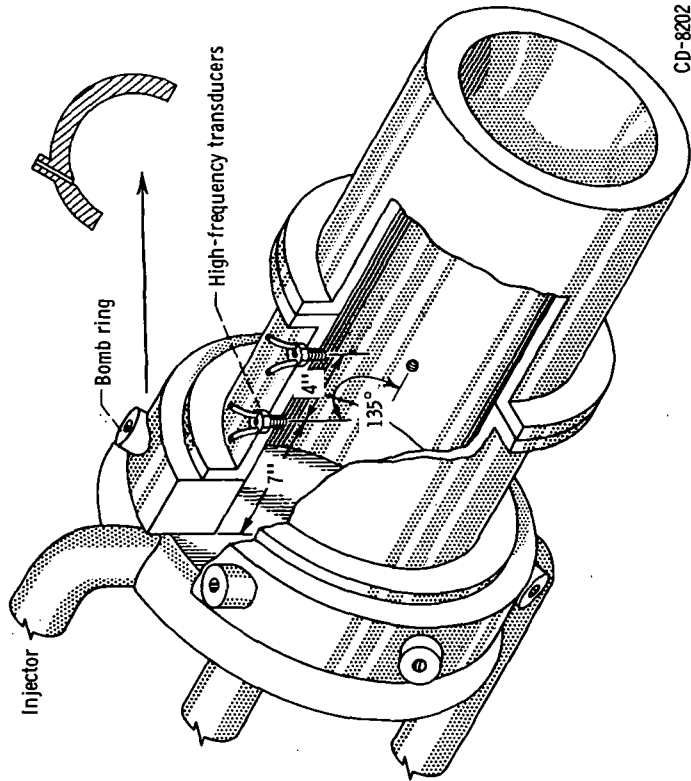
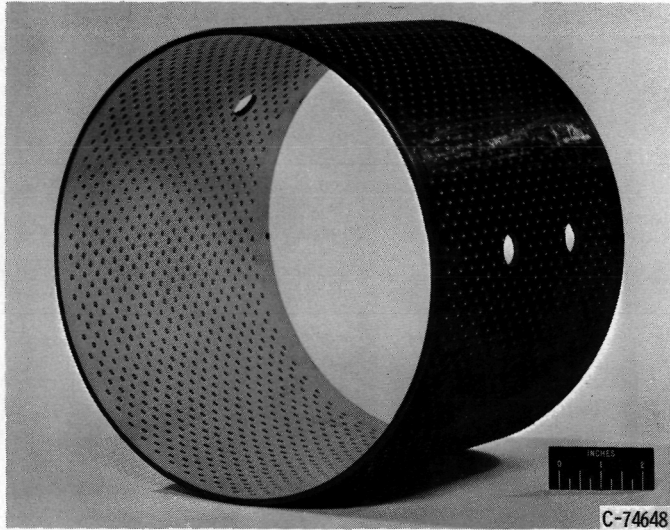
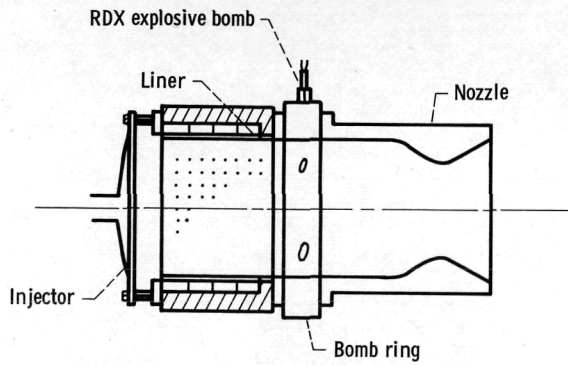


Figure 1. - Rocket combustor with bomb ring.

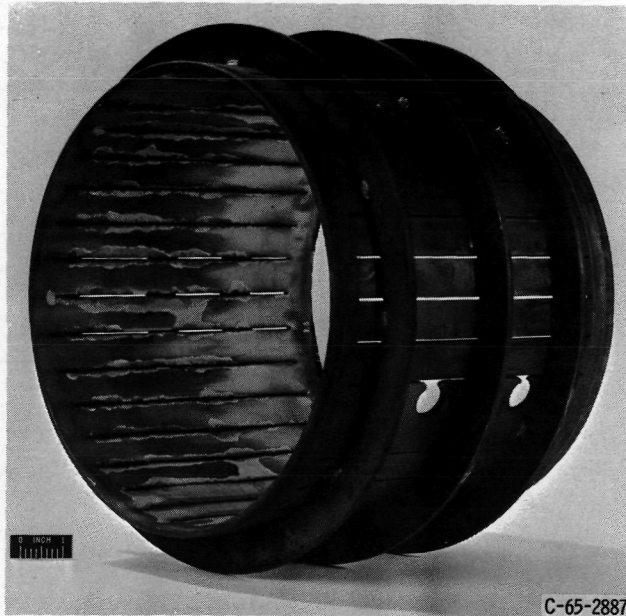


(a) Photograph.

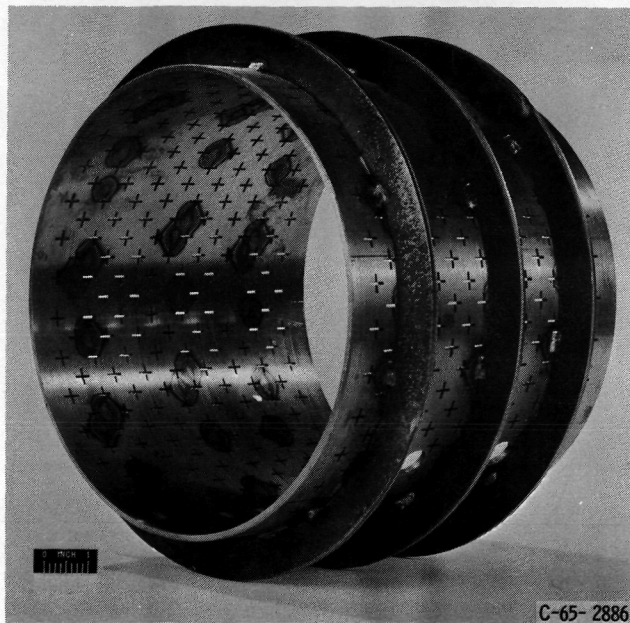


(b) Illustration.

Figure 3. - Perforated liner. Aperture diameter, 0.125-inch; thickness, 0.1875-inch; open area, 10 percent.

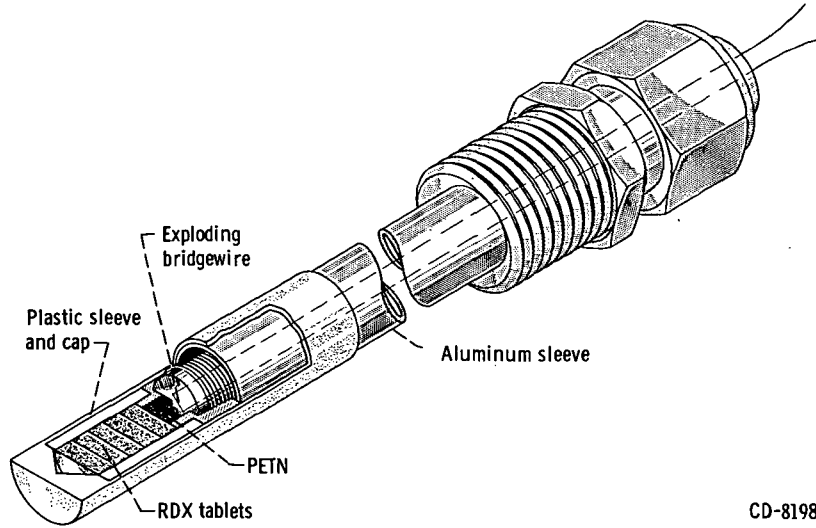


(a) Slot liner.



(b) Cross liner.

Figure 4. - Acoustic liners tested.



CD-8198

Figure 5. - RDX explosive bomb.

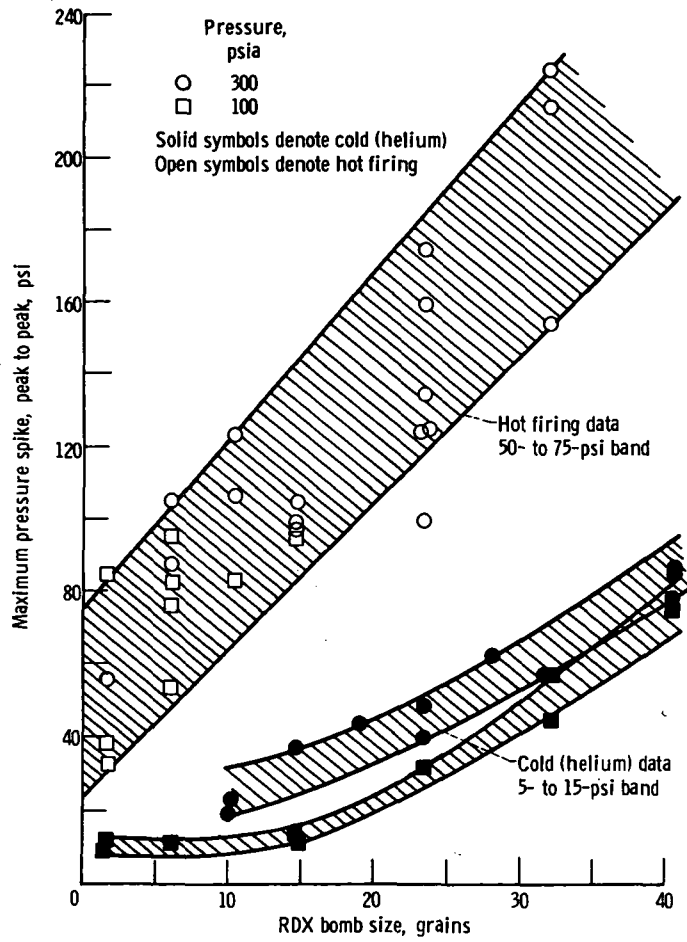


Figure 6. - RDX bomb data.

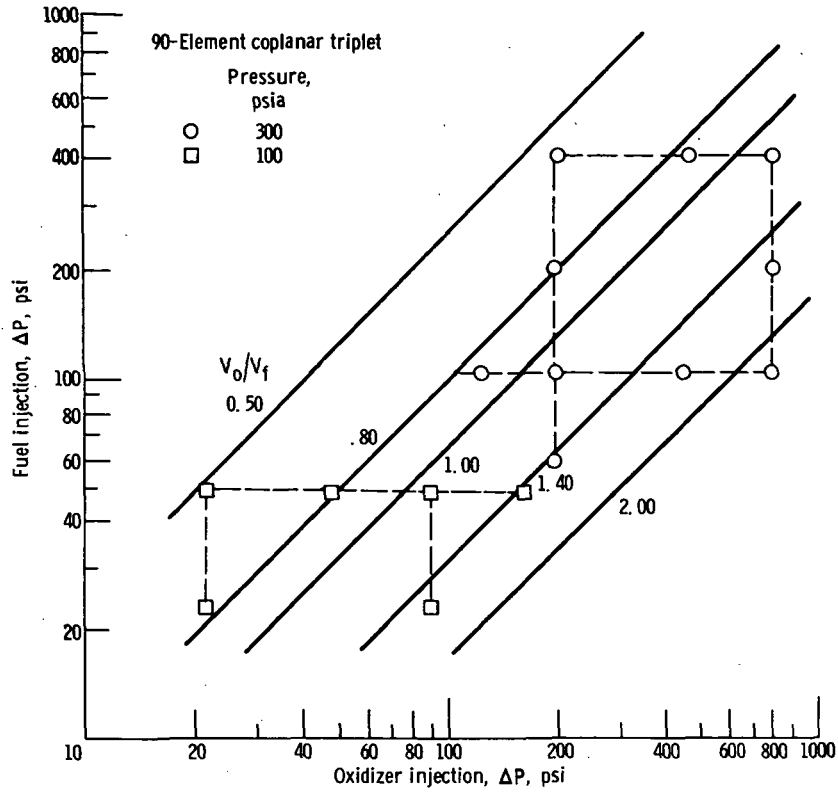


Figure 7. - Range of V_o/V_f tested.

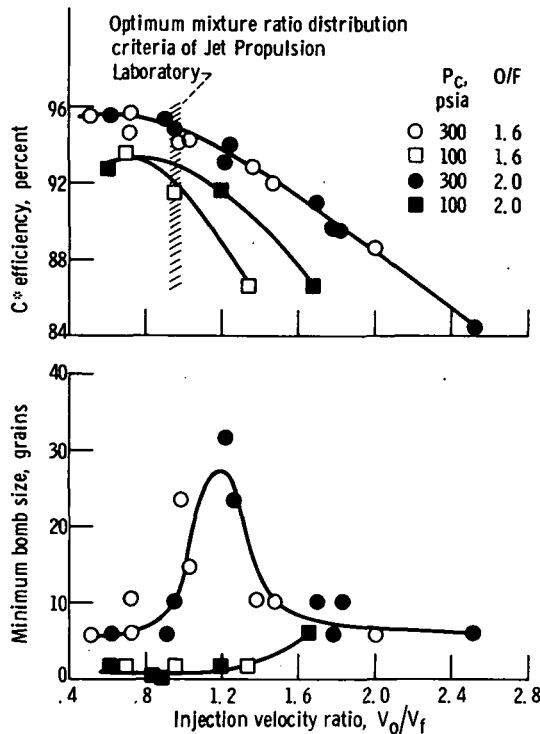


Figure 8. - Injection velocity ratio effect. Fuel-oxidant-fuel triplet; 90 elements; impingement, 60° , 0.5 inch.

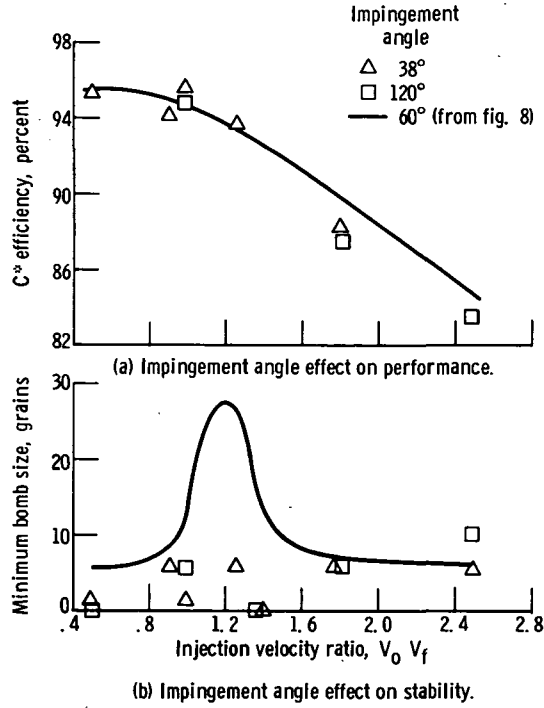


Figure 9. - Effect of impingement angle on stability and performance. Fuel-oxidant-fuel triplet; 90 elements; impingement, 0.5 inch; pressure, 300 psia; oxidant-fuel ratio, 2.0.

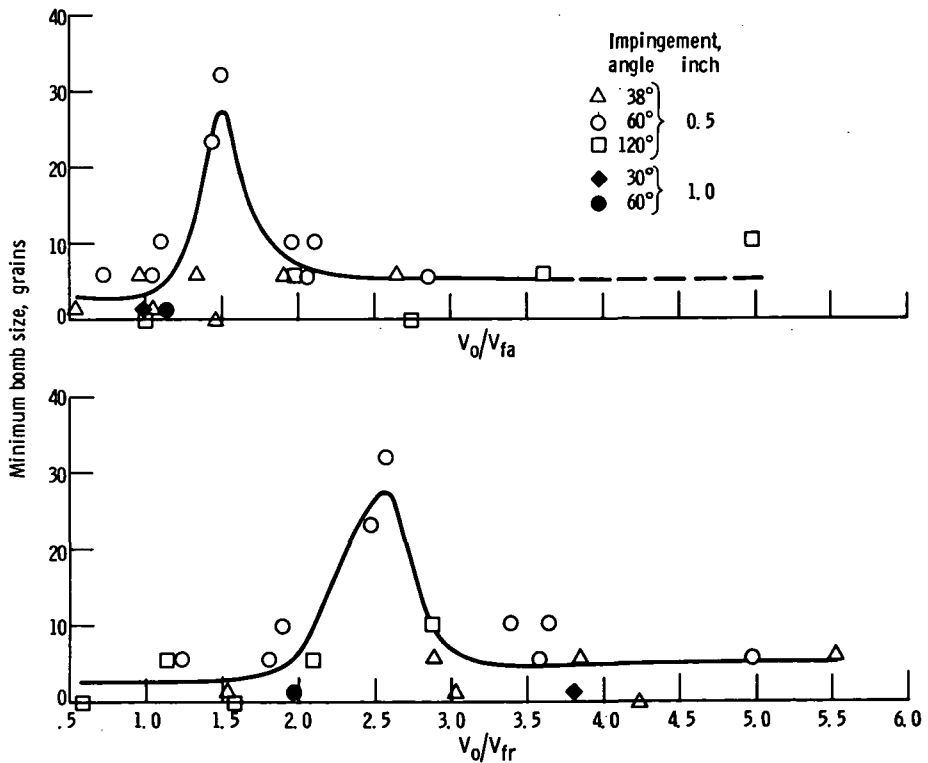


Figure 10. - Correlation of impingement angle and distance. Fuel-oxidant-fuel triplet; 90 elements; P_c 300 psia; oxidant-fuel ratio, 2.0.

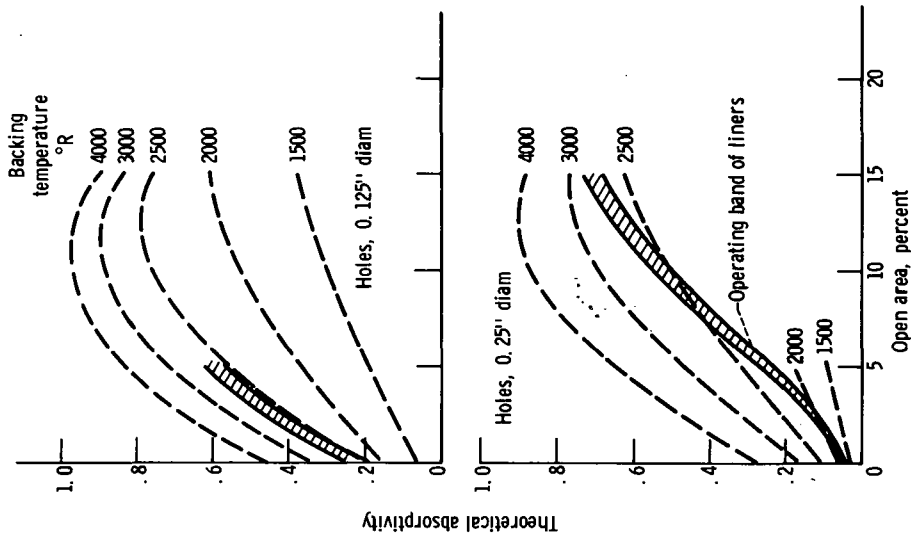
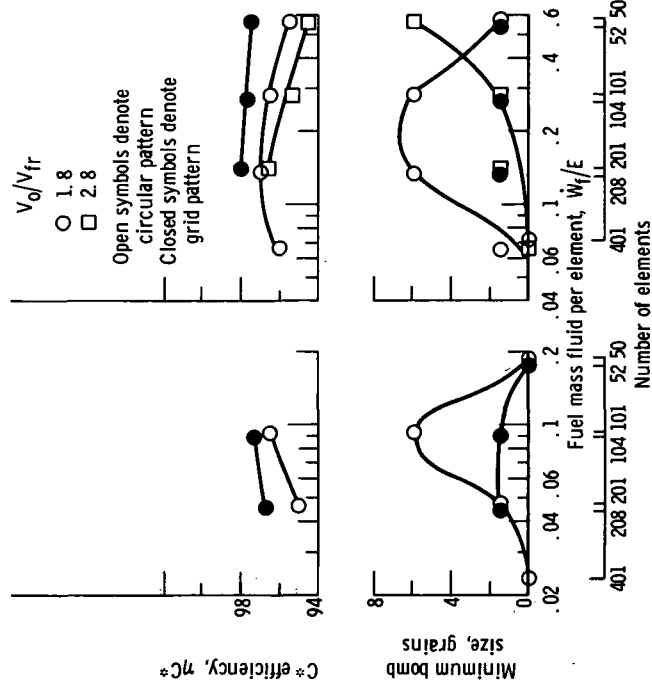


Figure 12. - Liner theoretical absorptivity. Frequency, 5000 cps.



(a) Chamber pressure, 100 psia. (b) Chamber pressure, 300 psia.
 Figure 11. - Effect of fuel mass flow per element (unstable performance data not plotted). Fuel-oxidant-fuel triplet; impingement, 60°, 0.5 inch; oxidant-fuel ratio, 2.0.